https://doi.org/10.5194/egusphere-2026-6044
Preprint. Discussion started: 5 November 2026
© Author(s) 2026. CC BY 4.0 License.

Ecohydrological coupling and episodic hydrological connectivity in the Edwards Plateau

Patricio N. Magliano,[1,2,3]* Pedro A. M. Leite,[4] Horia G. Olariu,[1] Bradford P. Wilcox[1]

1 – Department of Ecology and Conservation Biology, Texas A&M University, College Station, TX
2 – Grupo de Estudios Ambientales- IMASL, Universidad Nacional de San Luis (UNSL) y CONICET, San Luis, Argentina
3 – Departamento de Biología, Facultad de Química, Bioquímica y Farmacia, Universidad Nacional de San Luis, San Luis, Argentina
4 – Department of Environmental and Geospatial Science, Stephen F. Austin State University, Nacogdoches, TX

Abstract

In semiarid karst systems, the hydrologic budget is regulated by strong interactions among the water fluxes of precipitation, soil water dynamics, evapotranspiration, runoff, and groundwater recharge. In this study, we evaluated the temporal coupling among these fluxes in the Edwards Plateau Balcones Fault Zone (Texas, USA) using five years (2021–2025) of daily observations of precipitation (P), soil water content (SWC), evapotranspiration (ET), runoff (Rf), and groundwater (GW). Soil water content responses to precipitation exhibited threshold-dependent behavior under both dry and wet antecedent conditions, with breakpoints at 66.9 and 32.6 mm, respectively. Evapotranspiration dynamics were jointly controlled by SWC and temperature, with strong limitations under dry soil conditions and maximum ET values occurring only under warm and wet conditions. In contrast, Rf and GW responses were highly episodic and associated with the relatively rare large precipitation events. Although both fluxes increased rapidly following rainfall inputs, Rf responses were short-lived whereas GW responses persisted for several weeks to months. Groundwater recharge exhibited a clear threshold response, occurring only after precipitation events greater than 78 mm and never following events smaller than 62 mm. On the basis of these findings, we have developed a conceptual model for semiarid karst ecosystems whereby hydrological connectivity is activated during short-lived windows created only when precipitation pulses exceed both atmospheric demand and internal storage thresholds.

Keywords: aquifer, ecohydrology, karst soils, precipitation, rainfall, runoff, water table, water-limited environments.

*Corresponding author: pnmagliano@gmail.com

https://doi.org/10.5194/egusphere-2026-6044
Preprint. Discussion started: 5 November 2026
© Author(s) 2026. CC BY 4.0 License.

1. Introduction

Water fluxes in semiarid ecosystems are characterized by strong temporal variability in atmospheric inputs and tight coupling between climate, vegetation, and soil processes (Berdugo et al., 2020; Seneviratne et al., 2010; Reynolds et al., 2004). In these systems, precipitation (P) is highly variable, occurring as discrete pulses that must be rapidly partitioned among different fluxes, including evapotranspiration (ET), soil water content (SWC), runoff (Rf), and groundwater recharge (GW) (Magliano et al., 2026; Jobbágy et al., 2008; Huxman et al., 2004). Because potential ET exceeds rainfall, a large fraction of incoming water is returned to the atmosphere, limiting the amount of water available for subsurface fluxes (Olariu et al., 2025; Nosetto et al., 2020). As a result, SWC operates as a transient storage that mediates the redistribution of rainfall inputs over time (Chamizo et al., 2012; Vanderlinden et al., 2012; Zhao et al., 2007). Vegetation further modulates soil water dynamics by controlling ET rates and influencing infiltration through root structure and soil–plant interactions (Van Stan and Pinos, 2023; Whitworth-Hulse et al., 2023; Magliano et al., 2016). These dynamics can be interpreted through the lens of hydrological connectivity, whereby water fluxes are activated intermittently as thresholds are exceeded, rather than operating as continuous processes (Wilcox et al., 2022; Moreno-De-Las-Heras et al., 2020; Schwinning et al., 2004).

The Edwards Plateau of central Texas is a complex semiarid landscape wherein climatic variability, karst geology, and land management practices interact to shape hydrological processes (Heilman et al., 2014; Schwartz et al., 2013). The region is characterized by shallow, rocky soils overlying fractured limestone, which promotes rapid infiltration through preferential pathways while limiting soil water storage capacity (Leite et al., 2023, 2018; Heilman et al., 2009). The vegetation consists of mixed woody and herbaceous communities, including oak and juniper species, which exert strong control over infiltration rates (Leite et al., 2020), ET dynamics (Litvak et al., 2011; Heilman et al., 2009), and water use efficiency (Elkington et al., 2014). Over the past century, land use changes —particularly grazing practices— and woody plant encroachment have altered the region's vegetation structure and potentially modified the partitioning of rainfall between ET and Rf (Wilcox and Huang, 2010; Huxman et al., 2005). These biophysical alterations have resulted in a system in which water fluxes are highly sensitive to both atmospheric forcing and internal structural controls (Asbjornsen et al., 2011; Baldocchi et al., 2002). In particular, the combination of limited soil storage and high evaporative demand enhances the likelihood that rainfall from small events will be rapidly lost to ET, whereas larger events may trigger distinct hydrological responses (e.g., Rf generation, groundwater recharge) (Niborski et al., 2026; McMillan, 2020). Understanding how these factors interact is essential for interpreting water fluxes in semiarid karst regions and, in turn, for assessing the impact of various land management practices on hydrological functioning.

https://doi.org/10.5194/egusphere-2026-6044
Preprint. Discussion started: 5 November 2026
© Author(s) 2026. CC BY 4.0 License.

The Edwards Aquifer is one of the most important groundwater bodies in North America, supplying water to two millions people and supporting critical ecological and economic activities in central Texas (Sharp and Banner, 2018; Chen et al., 2001). Recharge to the aquifer occurs primarily within the Edwards Plateau Balcones Fault Zone, where surface water and infiltrating rainfall enter the karstic subsurface through fractures, conduits, and other preferential flow structures (Huang and Wilcox, 2005; Ferrill et al., 2004). However, recharge is highly variable in time and space, reflecting the episodic nature of rainfall and the complex interactions among surface and subsurface processes (Gregory et al., 2009; Scanlon et al., 2006). Historical droughts, particularly the severe drought of the 1950s, have demonstrated the vulnerability of the aquifer to prolonged deficits in recharge, with significant consequences for water availability and ecosystem functioning (Nielsen-Gammon et al., 2020; Loáiciga et al., 2000). Despite its importance, the processes governing when and how recharge occurs remain poorly understood. Addressing this knowledge gap is essential for improving predictions of aquifer response under changing climatic and land use conditions.

A key challenge in understanding recharge dynamics in karst systems lies in the coupling between ecohydrological fluxes operating across different temporal and spatial scales. P inputs are partitioned into different water fluxes (i.e., ET, Rf, and GW recharge) (Baker et al., 2021; Villegas et al., 2010; Hartmann et al., 2014). This partitioning is dynamically coupled through shared controls, including rainfall magnitude, antecedent soil moisture, and temperature (Morrissey et al., 2021; Canton et al., 2011). In this context, Rf and GW responses reflect episodic hydrological connectivity, whereby lateral and vertical fluxes are activated by rainfall events that exceed infiltration and/or storage capacity (Búrquez et al., 2024; Basant et al., 2020; Magliano et al., 2015; Chappell and Tych, 2012). For this reason, Rf and recharge arise from transient hydrological connectivity across spatial scales, from the soil profile to the catchment (Niborski et al., 2026; Castelli et al., 2019; Mayor et al., 2011). Capturing these dynamics requires moving beyond steady-state or averaged representations of the water cycle and focusing instead on event-scale processes and non-linear interactions (Figure 1).

https://doi.org/10.5194/egusphere-2026-6044
Preprint. Discussion started: 5 November 2026
© Author(s) 2026. CC BY 4.0 License.

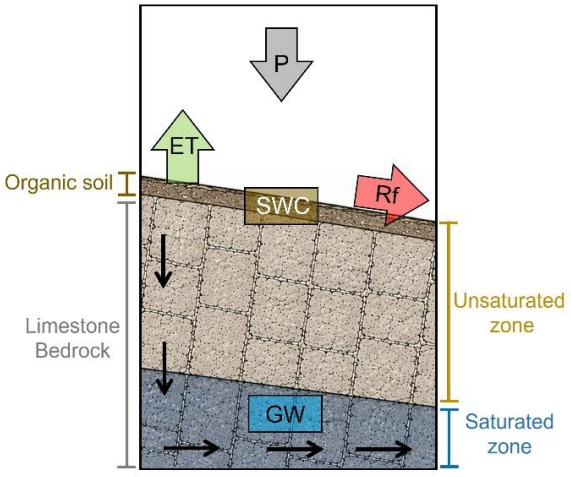


Figure 1. Conceptual model of hydrological fluxes and storage components in the Edwards Plateau: precipitation (P), soil water content (SWC), evapotranspiration (ET), surface runoff (Rf), and groundwater (GW). Black arrows show the movement of water through the fractured karstic bedrock (unsaturated zone; vertical movement) towards the unconfined groundwater level (saturated soil; lateral movement).

This study aims to characterize the ecohydrological coupling of water fluxes in the Edwards Plateau Balcones Fault Zone, with emphasis on the emergence of threshold-dependent vertical connectivity. Our specific objectives are to (i) identify the temporal coupling between water fluxes; (ii) evaluate how P inputs translate into SWC responses under contrasting antecedent moisture conditions; (iii) assess the controls of SWC and temperature on ET, to determine how atmospheric demand regulates water loss and modulates near-surface coupling; (iv) explore the temporal dynamics of Rf and GW recharge, focusing on its episodic nature and rapid activation; and (v) identify the P events that generate GW recharge processes. By integrating these components, we aim to determine how coupling strength varies across fluxes and conditions, and under which circumstances hydrological connectivity emerges in this karst system.

2. Methods

2.1 Study area

https://doi.org/10.5194/egusphere-2026-6044
Preprint. Discussion started: 5 November 2026
© Author(s) 2026. CC BY 4.0 License.

The study was conducted in the Field Research Park (29.66, −98.38), a 150-acre research and educational property managed by the Edwards Aquifer Authority (https://www.edwardsaquifer.org/aquifer-science/sustainability/frp/). It is located adjacent to Cibolo Creek on the Balcones Fault Zone of the Edwards Aquifer in northeast Bexar County, Texas, USA (Figure 2). The region is semiarid, characterized by strong climatic seasonality, shallow soils, and heterogeneous carbonate substrates, with spatially variable permeability and rapid infiltration occurring through fractures and other karst features (Fowler, 2005; Toomey III et al., 1993; Smeins, 1976). The mean annual precipitation is 767 mm, distributed irregularly throughout the year and dominated by high-intensity convective events, particularly during spring and early fall (Hernandez et al., 2014; Estaville and Earl, 2008). Potential ET generally exceeds rainfall, resulting in a water-limited system wherein atmospheric demand exerts a strong control on water fluxes (Heilman et al., 2009; Estaville and Earl, 2008). The soils, developed over Cretaceous limestone formations, are typically shallow, stony, and discontinuous with limited storage capacity and high spatial heterogeneity (Schwantes et al., 2017). The underlying karst geology is characterized by fractures, joints, and solutional features that facilitate rapid infiltration and preferential flow toward the subsurface, enhancing vertical and lateral connectivity during intense rainfall events (Toomey III et al., 1993; Smeins et al., 1976; Wilcox et al., 2008). The vegetation is dominated by a mosaic of oak–juniper woodlands and grasslands, where species such as *Juniperus ashei* and *Quercus spp*. play a key role in regulating ET and soil moisture dynamics (Wilcox et al., 2007, 2008). Land use in the region reflects a transition from historical overgrazing in the late 19th and early 20th centuries to recreation, real estate, and conservation. Beginning around the mid-20th century, reduced grazing pressure facilitated the expansion of juniper and oak woodlands (Archer et al., 2017; Wilcox et al., 2012). Today, much of the landscape, especially near urban areas, is dominated by woody vegetation, with likely consequences to hydrologic partitioning (Leite et al., 2025; Thurow & Hester, 1997; Wilcox et al., 2022).

https://doi.org/10.5194/egusphere-2026-6044
Preprint. Discussion started: 5 November 2026
© Author(s) 2026. CC BY 4.0 License.

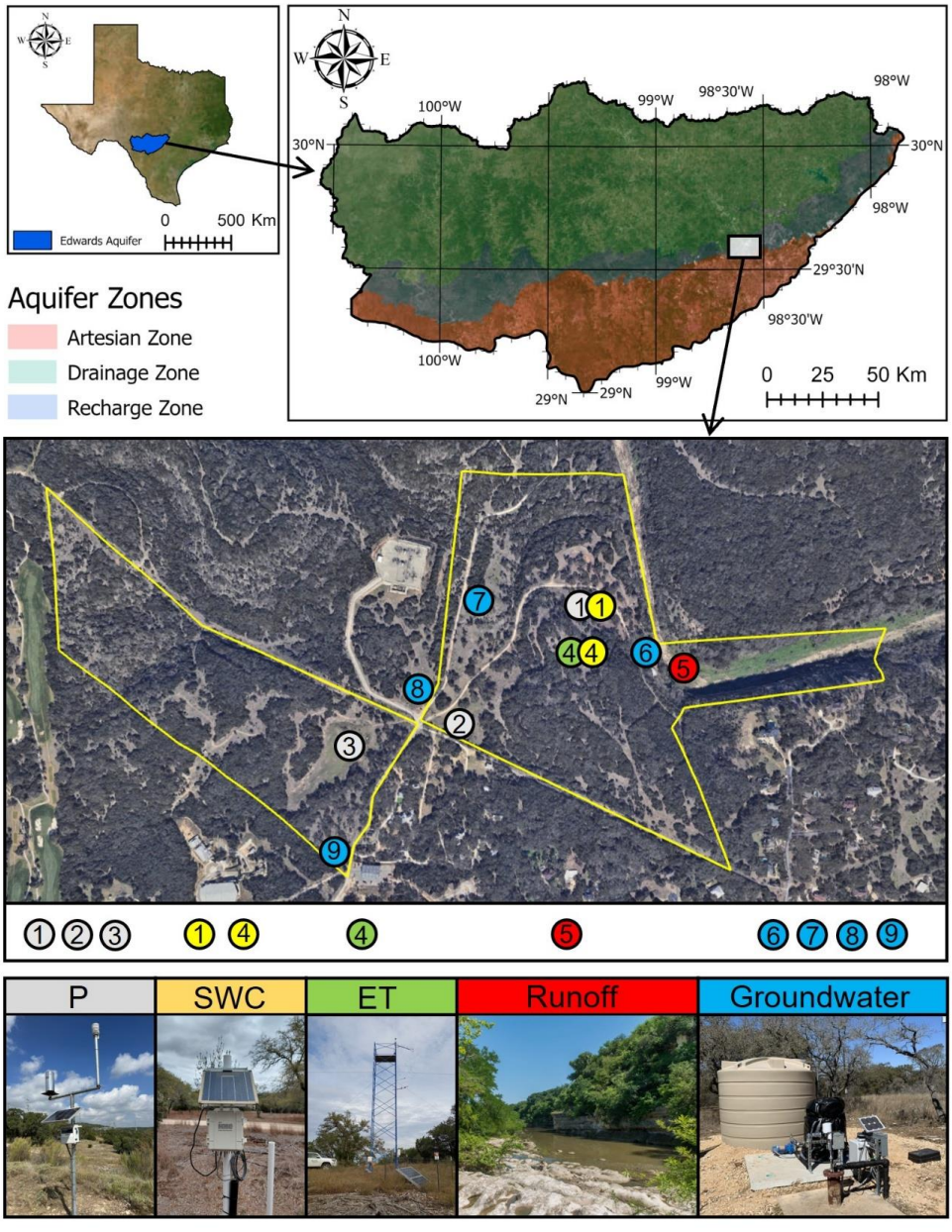


Figure 2. Location of the study area within the Edwards Plateau Balcones Fault Zone in central Texas. The upper panels show the location of the aquifer and its hydrogeologic subdivisions (artesian, drainage, and recharge zones), with the study site indicated. The middle panel presents a high-resolution aerial view of the study area (the Field Research Park is outlined in yellow with the monitoring locations denoted by colored circles). Aerial

https://doi.org/10.5194/egusphere-2026-6044
Preprint. Discussion started: 5 November 2026
© Author(s) 2026. CC BY 4.0 License.

imagery © 2026 Google; imagery © 2026 Landsat/Copernicus. The lower panel shows representative field installations for each flux measured: precipitation (P), soil water content (SWC), evapotranspiration (ET), runoff (Rf), and groundwater (GW).

2.2 Field measurements and data calculation

To address the specific objectives, we used data from the Edwards Aquifer Authority and the FLUXNET network. The time series ranged from 8 to 60 months, depending on the flux and the sensor. All raw data were recorded at sub-hourly intervals and subsequently aggregated to daily values. Precipitation data were summed, whereas air temperature, SWC, ET, Rf, and GW were averaged. The resulting daily time series exhibited overlap among fluxes, depending on sensor operation periods.

The P record spans 1,750 days, from 1 March 2021 to 15 December 2025. Precipitation (mm) was measured by means of electronic tipping-bucket rain gauges connected to Lufft WS502 weather stations. Measurements were recorded every 5 min and aggregated to daily totals by summation of the 288 readings taken per day. The P series was computed as the daily average of three rain gauges (Figure 2). Pairwise linear correlations among gauges were evaluated via Spearman correlation coefficient; all correlations were positive and statistically significant ($p < 0.01$). Air temperature (°C) was processed analogously by computing daily averages from 5-min observations.

The SWC record spans 1,750 days, from 1 March 2021 to 15 December 2025. Soil water content (%) was measured with soil moisture sensors RXW-T12-900 (Hobo Onset) at two sites (one profile of 0–30 cm deep per site). Data were recorded every 5 min and aggregated to daily values by averaging the 288 measurements per day. The SWC series corresponds to the daily mean of the two sites. Spearman correlation analysis indicated a positive and significant relationship between both sites ($p < 0.01$).

The ET record spans 1,502 days, from 4 March 2021 to 14 April 2025. Evapotranspiration (mm) was quantified by means of an eddy covariance tower installed at the Field Research Park. The system consists of a three-dimensional sonic anemometer (CSAT-3, Campbell Scientific, Logan, UT, USA) and an open-path infrared gas analyzer (LI-7500, LI-COR, Lincoln, NE, USA), mounted 4 m above the dry forest canopy. The instruments measure wind velocity components, sonic temperature, and CO_2 and H_2O vapor concentrations. Data were sampled at 20 Hz and logged via a CR1000 datalogger (Campbell Scientific, Logan, UT, USA). High-frequency data were processed and aggregated to daily ET totals. Analyses involving ET were restricted to periods with available data. The LI-7500 sensor was non-

https://doi.org/10.5194/egusphere-2026-6044
Preprint. Discussion started: 5 November 2026
© Author(s) 2026. CC BY 4.0 License.

operational between 20 January and 8 March 2022, and between 24 January and 26 March 2024.

Runoff was measured in one watershed **(**Cibolo Creek**,** lat-lon: 29.6626340, −98.3787590) and spans 1,750 days (1 March 2021 to 15 December 2025). Stream stage was recorded every 15 min with a pressure transducer (HOBO U-20-L, Onset). Daily discharge (see below) was computed as the mean of sub-daily discharge estimates, which approximates the time-integrated flux under quasi-steady daily conditions (96 measurements per day). Stream discharge (i.e., Rf) at Cibolo Creek was estimated with the velocity–area method, based on continuous stage measurements (Rantz et al., 1982; Turnipseed and Sauer, 2010). Water level was recorded by a fixed sensor located at the lowest point of a surveyed cross section. To capture the irregular geometry of the channel, the cross section was surveyed in the field via a series of discrete elevation measurements along the channel transect. The resulting survey points were then used to numerically derive the stage–area relationship. Stage values were converted to flow depth relative to the channel thalweg. The wetted cross-sectional area (A(h)) corresponding to each stage value was computed by numerical integration of the submerged portion of the surveyed elevation profile, by means of the trapezoidal rule:

$$A(h) = \Sigma\, [(y_i + y_{i+1}) / 2] * (x_{i+1} - x_i)\ , \qquad (1)$$

where y_i is the maximum height (0, h − z_i—z_i being the bed elevation at horizontal coordinate), x_i is the horizontal position along the surveyed cross section, and h is the instantaneous water level relative to the channel thalweg.

Daily discharge was computed as the mean of sub-daily discharge estimates, which approximates the time-integrated flux under quasi-steady daily conditions. Specifically, discharge was calculated as:

$$Q(t) = A(h_t) * V\ , \qquad (2)$$

where V represents a characteristic mean flow velocity. In the absence of contemporaneous velocity measurements, a representative constant velocity was adopted based on the range of reported mean velocities for streams under moderate flow conditions observed in limestone-bed rivers of the Edwards Plateau (Gustavson 1978). Daily Rf yield ($m^3\ day^{-1}\ ha^{-1}$) was calculated by normalizing discharge from the contributing watershed area:

$$Rf\ yield = Qd / A\ , \qquad (3)$$

where Qd is daily discharge ($m^3\ day^{-1}$) and A is the watershed area (11,576 ha)

https://doi.org/10.5194/egusphere-2026-6044
Preprint. Discussion started: 5 November 2026
© Author(s) 2026. CC BY 4.0 License.

Groundwater level (m a.s.l.) was measured at four monitoring wells for periods ranging from 669 to 1,729 days, depending on date of installation, with all records ending on 15 December 2025. Each well was instrumented with an OTT PLS500 pressure transducer that records water level every 15 min. Daily groundwater levels were calculated by averaging the 96 measurements per day. Then, daily values of the four wells were averaged to obtain a single robust temporal series, and values were referenced to the surface (m from the surface level).

2.3 Statistical analysis

We determined the temporal dynamics pattern of each flux and the coupling between them by constructing cumulative distributions of P, ET, SWC, runoff, and GW. We first normalized daily time series of each flux by its total cumulative sum over the study period (2021–2025), which yielded dimensionless values ranging from 0% to 100%. Then, to preserve the discrete nature of the observations and highlight episodic contributions, we converted the normalized series to cumulative percentages and plotted them day by day. In the case of ET, missing data (less than 7% of the complete series) was filled by the average of ET data for the same calendar days of the other years.

We determined relationships between P events and changes in SWC (SWC increment, %) by separating observations according to antecedent moisture conditions: dry soil (SWC < 15%) and wet soil (SWC > 15%). For each subset, we modeled the relationship between P event size (mm) and SWC increment (%) using a piecewise linear regression constrained to pass through the origin (Niborski et al., 2026; Gnatowski et al., 2018). The model consisted of a first segment with a positive slope up to a threshold value, followed by a second segment with zero slope, representing a plateau. We estimated the breakpoint (threshold) by minimizing the residual sum of squares of candidate values (those within the central range of observed P events) (Shao et al., 2022). To evaluate the model's performance, we used the coefficient of determination (R^2) and assessed statistical significance at $p < 0.01$.

We determined the response of ET as a function of mean air temperature (T) and SWC by fitting a generalized additive mixed model (GAMM) to ET actual data (Zuur 2009). This model takes into account non-linear effects and temporal dependence, as follows:

$$ET_t = s_1(T_t) + s_2(SWC_t) + s_3(Time_t) + \varepsilon_t, \quad (4)$$

where ET_t is daily ET at time t; s_1, s_2, and s_3 are cubic regression splines for T, SWC, and time, respectively; T_t is daily air temperature at time t; SWC_t is daily SWC at time t; $Time_t$ is the number of days since the beginning of the record, included to capture seasonal variability and long-term trends; and ε_t is the residual error term, modeled as a first-order

https://doi.org/10.5194/egusphere-2026-6044
Preprint. Discussion started: 5 November 2026
© Author(s) 2026. CC BY 4.0 License.

autoregressive process, $\varepsilon_t=\rho\varepsilon_{(t-1)}+u_t$, where ρ is the lag^{-1} autocorrelation parameter and u_t is an independent error term.

We fitted the model assuming a gaussian error distribution with identity link and selected spline basis dimensions that would provide sufficient flexibility to capture non-linear responses while avoiding overfitting. Finally, we evaluated the adequacy of the model using residual diagnostics, including inspection of autocorrelation functions, and applied Durbin–Watson statistics and Ljung–Box tests to whitened residuals. The smoothed temporal term effectively captured seasonal variability, while the AR(1) structure reduced residual autocorrelation (Durbin–Watson ≈ 2 for whitened residuals), indicating that the estimated relationships represent process-level controls rather than artifacts of shared seasonal structure.

For Rf (mm) and GW (m from surface), we analyzed dynamics using continuous time series. To facilitate comparison, we normalized both fluxes to a relative scale (0–100) using min–max transformation. Then, to explore event-scale dynamics, we selected four representative situations of P–Rf–GW events on the basis of their magnitude and temporal isolation within the full record. For each situation, we defined time windows that would capture the complete hydrological response, including rising limb, peak discharge, and recession phase.

To identify which P events from the continuous time series were able to generate GW recharge, we defined an event as one separated from other events by at least 24 h without precipitation (Dunkerley, 2021). For each event, total P depth (mm) was calculated as the cumulative precipitation over its duration. All events were ranked by magnitude and plotted as a function of event size. They were then classified according to their hydrological response, distinguishing between those that generated a detectable increase in the water table (ΔGW > 0) and those that did not. Lastly, a transition zone was defined empirically as the interval during which an overlap in rainfall event size (both response classes occurring) was observed. Specifically, the lower limit was set as the smallest P event that generated a GW response, and the upper limit as the largest P event that did not generate a GW response.

3. Results

The analyzed fluxes exhibited contrasting temporal dynamics over the study period, reflecting differences in the timing, magnitude, and persistence of ecosystem water responses (Figure 3). Precipitation events of highly variable magnitude occurred throughout the record and were superimposed on a marked seasonal cycle in air temperature, with warm conditions concentrated during summer months and cooler conditions during winter. Soil water content responded rapidly to P pulses, with abrupt increases frequently reaching

https://doi.org/10.5194/egusphere-2026-6044
Preprint. Discussion started: 5 November 2026
© Author(s) 2026. CC BY 4.0 License.

25%–30%, followed by relatively rapid declines during dry periods. Evapotranspiration values displayed a pronounced seasonal pattern closely associated (with a two-month delay) with temperature and generally ranged from near zero during winter to peaks approaching 6 mm day^{-1} during warm periods. In contrast, Rf dynamics were strongly episodic, characterized by infrequent but pronounced peaks separated by extended periods of negligible flow. The largest Rf events occurred during 2021 and 2025, whereas most of the record remained near baseline conditions. Groundwater levels exhibited substantially smoother and more persistent dynamics than surface fluxes—with abrupt rises following major hydrological events and recession phases extending over weeks to months—but displayed synchronous temporal behavior with Rf in terms of baseline levels, peak magnitudes, and recession trajectories. Overall, the time series reveal the coexistence of relatively continuous near-surface dynamics (SWC and ET) and highly episodic Rf and GW responses, suggesting distinct but temporally coupled hydrological pathways within the Balcones Fault Zone.

https://doi.org/10.5194/egusphere-2026-6044
Preprint. Discussion started: 5 November 2026
© Author(s) 2026. CC BY 4.0 License.

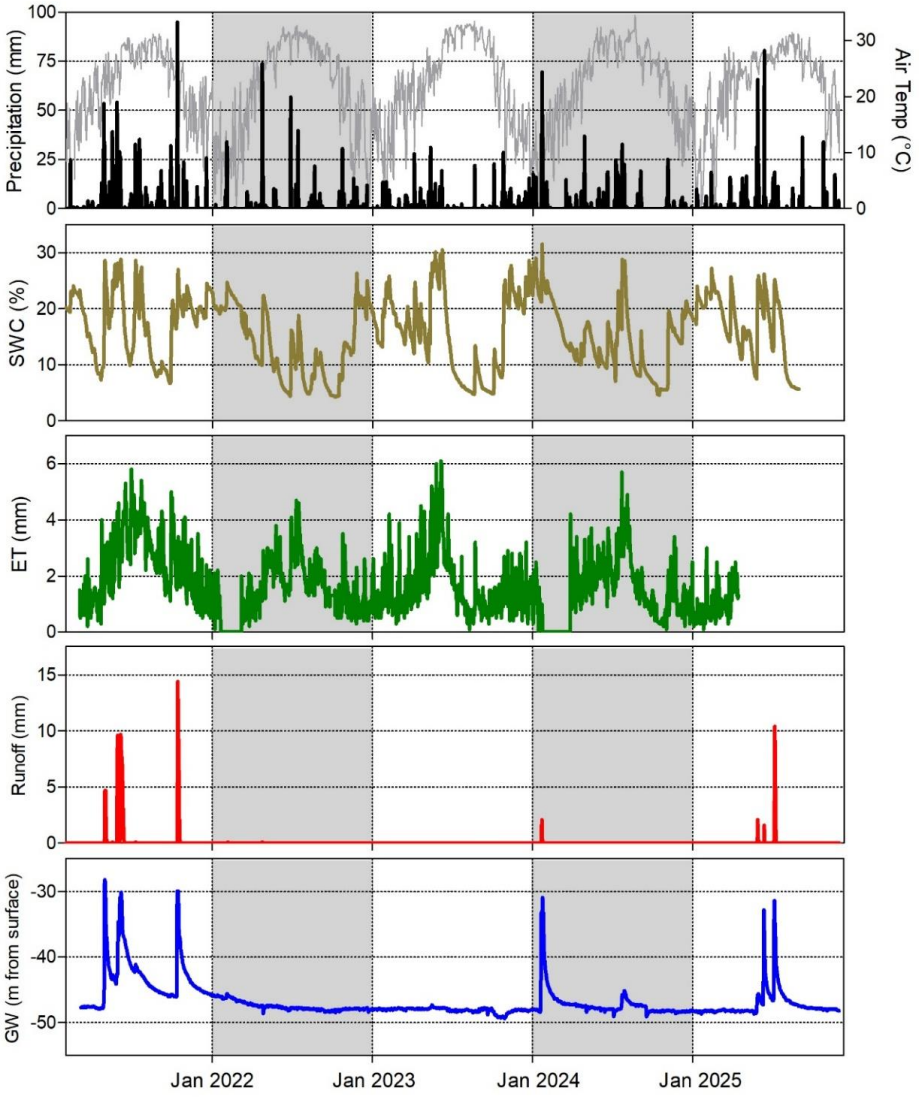


Figure 3. Time series of water fluxes in the Edwards Plateau. From top to bottom, panels show daily precipitation (P; left vertical axis) and mean daily air temperature (T; right vertical axis); soil water content (SWC); evapotranspiration (ET); Rf; and groundwater (GW) level. Alternating shaded and white bands indicate 12-month periods.

There were also clear differences in the temporal progression of the analyzed fluxes (Figure 4). Precipitation exhibits a relatively smooth and continuous increase over the study period, reaching 50% of its cumulative total by mid 2023 and approaching 100% in late 2025. In

https://doi.org/10.5194/egusphere-2026-6044
Preprint. Discussion started: 5 November 2026
© Author(s) 2026. CC BY 4.0 License.

contrast, Rf and GW display step-like patterns characterized by abrupt increases associated with discrete events, followed by extended periods with little or no change. Rf shows major increments early in the record (2021–2022), reaching approximately 65% of its cumulative total within the first year, then remains nearly constant until a second increase in early 2024 and another rise in 2025. Groundwater follows a similar but more delayed pattern, with marked increases occurring after Rf steps, particularly around early 2022, early 2024, and mid 2025. Soil water content and ET exhibit intermediate behavior: cumulative increases are more gradual than those of Rf and GW but accelerate noticeably during specific periods. The two fluxes track each other closely throughout the record, with SWC generally exceeding ET during the latter half of the study period. In sum, the timing and shape of the cumulative curves highlight distinct temporal patterns among fluxes, with continuous accumulation for P, SWC, and ET, and more episodic contributions for Rf and GW.

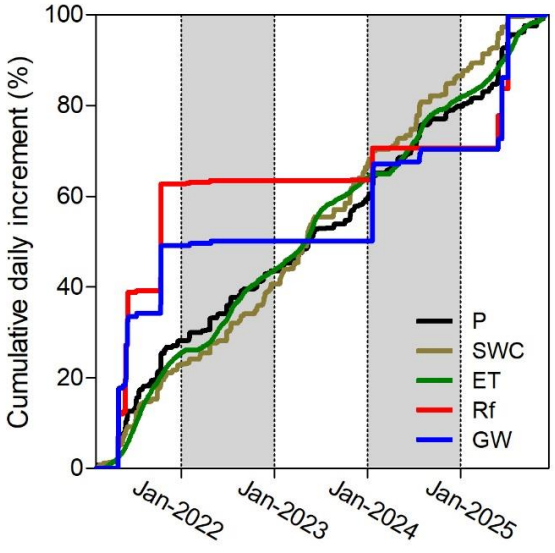


Figure 4. Cumulative daily increment curves for precipitation (P), soil water content (SWC), evapotranspiration (ET), runoff (Rf), and groundwater (GW) over the study period (2021–2025). Each time series was normalized by its total cumulative sum over the study period, which yielded dimensionless values ranging from 0% to 100%.

The relationship between P event magnitude and SWC increment differed markedly between dry and wet antecedent soil conditions (Figure 5). In both cases, the piecewise linear model constrained through the origin provided significant fits ($p < 0.01$), revealing threshold-dependent responses in SWC dynamics. Under dry soil conditions, SWC increment increased linearly with P up to a threshold of 66.9 mm, with a slope of 0.24%

https://doi.org/10.5194/egusphere-2026-6044
Preprint. Discussion started: 5 November 2026
© Author(s) 2026. CC BY 4.0 License.

SWC increase per mm of precipitation. Beyond this threshold, responses approached a plateau near 16.5% SWC increment. The overall model fit yielded an R^2 of 0.67. Under wet soil conditions, SWC increment also increased linearly with P, but the threshold occurred at a substantially lower P magnitude (32.6 mm), with a similar slope (0.25% per mm of precipitation). In this case, the response rapidly approached a lower plateau of approximately 7.9% SWC increment, and the model fit was stronger (R^2 = 0.89). Both antecedent moisture conditions exhibited non-linear and threshold-dependent responses, although dry soils required larger P events to reach saturation and displayed greater maximum SWC increments than wet soils.

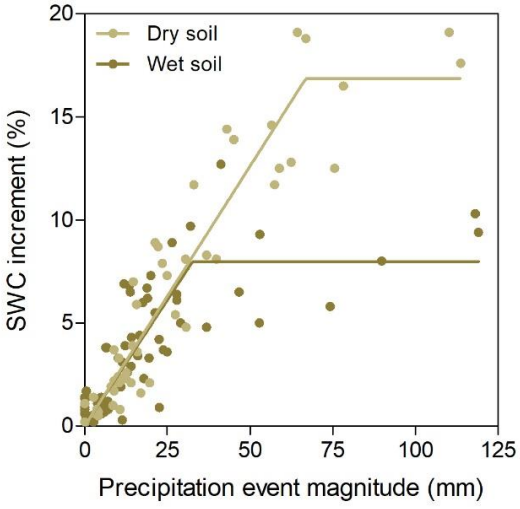


Figure 5. Soil water content (SWC) increment as a function of P event magnitude under contrasting antecedent moisture conditions. Data were fitted by means of piecewise linear models constrained to pass through the origin, with a positive slope up to a threshold and a zero slope (plateau) thereafter.

Both mean daily air temperature (T) and SWC exerted non-linear controls on daily ET dynamics (Figure 6). The response surface showed that predicted ET values ranged from near 0 mm day^{-1} under dry (<8% SWC) conditions to more than 4 mm day^{-1} under warm (15°–20°C) and wet (>25% SWC) conditions. Across the observed range of soil moisture, ET increased monotonically with SWC, displaying a pronounced inflection around 8%–10% SWC followed by a marked increase at higher moisture levels—indicating strong limitations on ET under dry soil conditions. The temperature response was also non-linear and positive, with ET remaining low at cooler temperatures and increasing progressively as temperatures rose. Changes in response slope became evident around 15°–20°C, beyond which ET

https://doi.org/10.5194/egusphere-2026-6044
Preprint. Discussion started: 5 November 2026
© Author(s) 2026. CC BY 4.0 License.

values increased more rapidly. The highest ET rates were observed under the combined occurrence of medium-to-high temperatures and elevated SWC, indicating strong interactive controls between atmospheric demand and soil water availability.

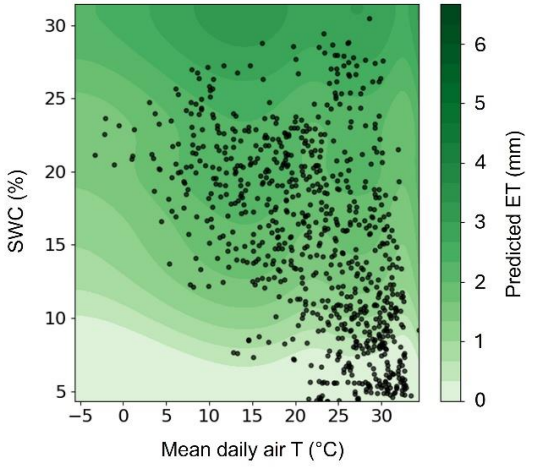


Figure 6. Response surface of daily ET (mm) as a function of mean daily air (T; °C) and SWC (%), as predicted by a generalized additive mixed model (GAMM). The green shading surface indicates predicted ET, with darker green tones representing higher values.

With respect to Rf and GW, responses generated by P events were strongly coupled but temporally asymmetric throughout the study period (Figure 7). In the four selected P–Rf–GW situations described earlier, both Rf and GW increased rapidly following P inputs—a near-synchronous onset of both responses within approximately one day of the main P pulse—indicating that surface and subsurface fluxes were triggered by the same P event. At the same time, the magnitude and persistence of the two responses differed markedly. Rf exhibited sharp, short-lived peaks, frequently reaching high relative values but returning rapidly toward baseline conditions within a few days. In contrast, while GW also increased abruptly and often reached similarly high relative values, it receded much more slowly—over several weeks to months—long after the Rf response had dissipated.

Figure 7 shows the Rf events in the four selected P–Rf–GW situations (representing the four large-magnitude P events that generated the greatest responses). These Rf responses displayed substantially greater variability in peak magnitude than the GW responses, whose peak magnitudes were largely independent of P-event magnitude and consistently remained within a relatively narrow range (~75%–100%). For example, Rf event (2) reached its maximum within one day of peak P and declined rapidly thereafter, whereas GW peaked shortly after peak P and remained elevated for 20–30 days. A similar pattern was observed

https://doi.org/10.5194/egusphere-2026-6044
Preprint. Discussion started: 5 November 2026
© Author(s) 2026. CC BY 4.0 License.

for Rf event (3): a moderate Rf pulse (~30%) coincided with a broader GW response (~80%), then receded gradually. Rf events (1) and (4) showed more complex, multi-pulse behavior, with repeated Rf peaks associated with successive P inputs and corresponding step-like increases in GW. In sum, Rf and GW are closely aligned in activation timing but differ strongly in response duration: Rf behaves as a rapid, transient flux, whereas GW integrates the event signal over longer timescales. This pattern supports the interpretation that large P events simultaneously activate lateral Rf pathways and vertical subsurface connectivity, but that GW storage dampens and prolongs the hydrological response.

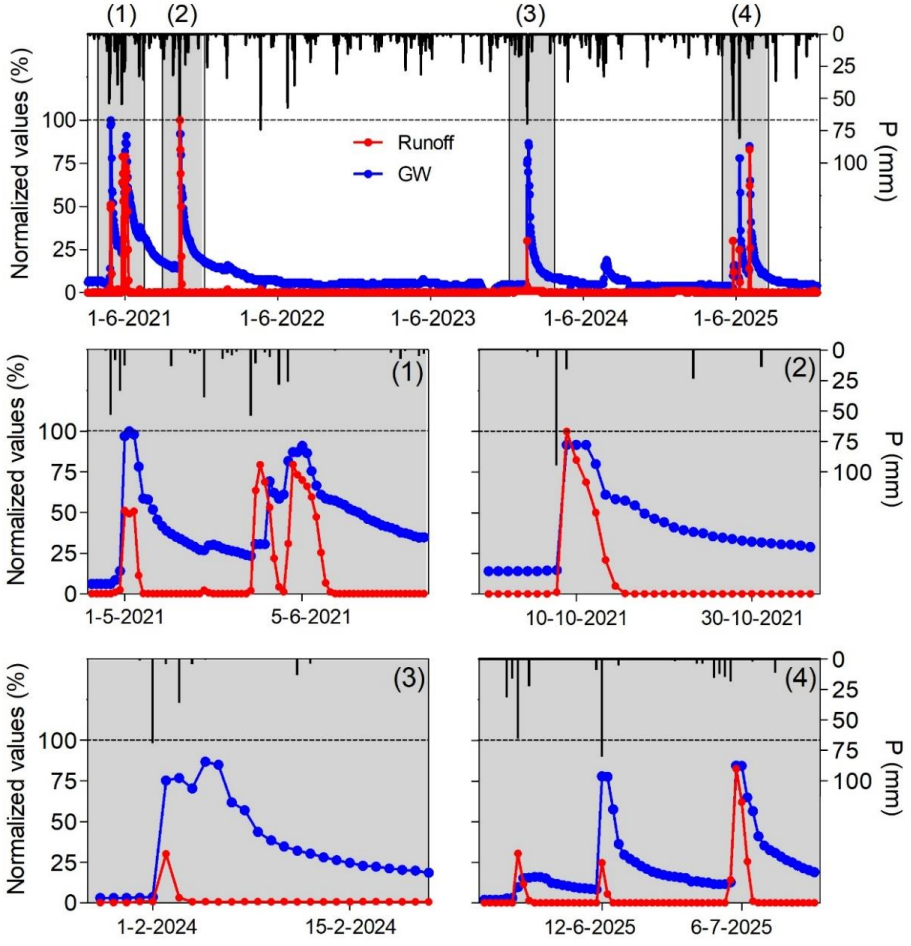


Figure 7. Normalized temporal dynamics of Rf and GW response from 2021 to 2025, as derived from measurements of the four selected P–Rf–GW situations. The upper panel shows the complete time series, with precipitation represented by the black vertical bars. The middle and lower panels show detailed pictures of the temporal coupling between precipitation, runoff generation, and groundwater response.

https://doi.org/10.5194/egusphere-2026-6044
Preprint. Discussion started: 5 November 2026
© Author(s) 2026. CC BY 4.0 License.

The P events exhibited a highly asymmetric distribution of magnitudes, with most not exceeding ~20 mm and only a limited number of large events (100–120 mm) (Figure 8). Clear differences emerged between events that generated detectable GW responses and those that did not. Most P events below 62 mm were not associated with measurable GW recharge, indicating that small and moderate events were generally insufficient to activate vertical hydrological connectivity. In contrast, all events exceeding 78 mm consistently generated GW responses, suggesting the existence of an upper threshold above which recharge systematically became activated. Between these two ranges (62–78 mm), a transition zone was observed in which both responsive and non-responsive behaviors occurred; that is, under intermediate precipitation magnitudes connectivity may or may not be activated. Recharge-generating events represented only a small fraction of the total number of P events and corresponded almost exclusively to the upper tail of the event magnitude distribution. The separation between responsive and non-responsive events was visually distinct, with minimal overlap between classes, yielding a clear stratification of P events into non-recharge-generating (<62 mm), transitional (62–78 mm), and consistently recharge-generating (>78 mm) categories based on P event magnitude.

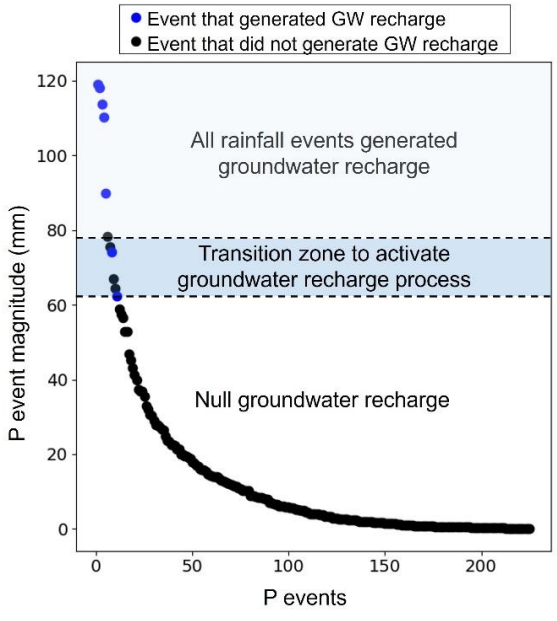


Figure 8. Distribution of P event magnitude and their role in generation of groundwater recharge. Each point represents an individual P event, classified according to whether it generated a detectable groundwater response (blue) or not (black). The shaded band

https://doi.org/10.5194/egusphere-2026-6044
Preprint. Discussion started: 5 November 2026
© Author(s) 2026. CC BY 4.0 License.

highlights the transition zone within which vertical hydrological connectivity may or may not be activated.

4. Discussion

In this study, we developed a process-based framework for understanding GW recharge in semiarid karst systems as an emergent property of pulse-driven ecohydrological dynamics. The water flux dynamics and coupling found are consistent with those of conceptual models developed for dryland ecosystems, wherein water movement is governed by non-linear responses to discrete P events and constrained by strong losses via ET (Berdugo et al., 2020; D'Odorico et al., 2013; Maestre et al., 2016; Wang et al., 2012; Ludwig et al., 2005). Our framework extends those earlier findings by explicitly linking soil moisture thresholds and ET dynamics to the activation of subsurface fluxes (Figures 5 and 6). In addition, it indicates that hydrological connectivity in this system is not persistent but event-driven, emerging only when climatic forcing and internal thresholds align (Figures 7 and 8). This perspective moves beyond traditional interpretations of recharge as a function of mean climate and instead emphasizes the role of event-scale processes and threshold behavior in regulating water fluxes.

We identified two distinct hydrological pathways: one continuous and dominated by soil water–atmosphere exchange, and another episodic and associated with Rf and recharge (Figure 9). Precipitation represents the primary atmospheric input and is partitioned among competing pathways depending on antecedent soil moisture, event magnitude, and substrate permeability. A fraction of incoming water infiltrates the soil profile, increasing SWC, which acts as a transient storage reservoir (Zhang et al., 2024; McDowell et al., 2023). From this storage, water may return to the atmosphere through ET. When P intensity exceeds infiltration capacity, or when SWC approaches saturation thresholds, lateral connectivity is activated, generating surface Rf. At the same time, vertical preferential flow associated with macropores, fractures, and karst features facilitate rapid percolation toward GW depth, bypassing much of the soil and bedrock matrix (McDowell et al., 2023; Saco et al., 2020). These preferential pathways enhance recharge efficiency by transmitting water pulses directly to depth (Hervé-Fernández et al., 2016; Gregory et al., 2009). Together, these flux regimes are dynamically coupled and regulated by P inputs and T seasonality (Calvo-Cases et al., 2021; Litvak et al., 2011)—reinforcing the idea that hydrological connectivity in semiarid karst landscapes is both episodic and scale-dependent (McDowell et al., 2023; Turnbull et al., 2008; Wilcox et al., 2008, 2003).

Importantly, water fluxes assessed in this study are connected not only at the landscape scale but also at regional scales. Lateral connectivity within the contributing zone routes Rf toward losing stream channels in the Balcones Fault Zone, where vertical connectivity is

https://doi.org/10.5194/egusphere-2026-6044
Preprint. Discussion started: 5 November 2026
© Author(s) 2026. CC BY 4.0 License.

rapidly activated (Scanlon et al., 2006). In karst systems, this coupling operates over much shorter timescales than in non-karst landscapes, enabling rapid transmission losses through discrete recharge features (Green et al., 2014; Hervé-Fernández et al., 2016). As a result, local GW-level responses may be disproportionately large relative to rainfall depth, reflecting integrated inputs over the entire contributing zone (Ford & Williams, 2007). Such regional-scale coupling between lateral and vertical connectivity helps explain the magnitude and timing of GW responses observed during our study.

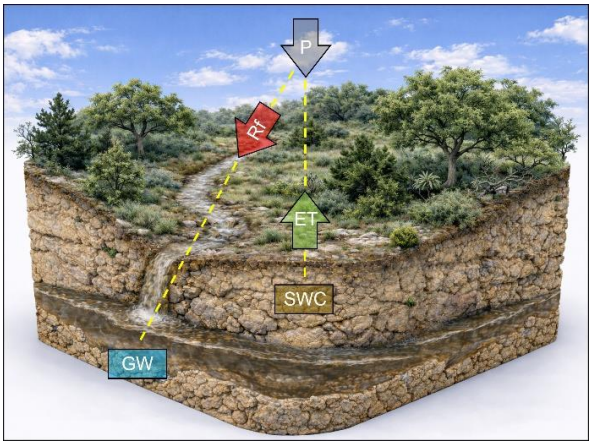


Figure 9. Conceptual model of precipitation partitioning and hydrological connectivity in a karst recharge system. Precipitation (P) is partitioned between surface runoff (Rf), evapotranspiration (ET), soil water storage (SWC), and percolation toward groundwater (GW). Dashed lines illustrate vertical and lateral preferential flow pathways activated under threshold conditions.

Our results can be interpreted within the ecohydrological coupling framework proposed by McDowell et al. (2023), which emphasizes that the degree of coupling among water fluxes depends on the hydraulic connectivity between source water pools and their partitioning into different fluxes. In our study area, the coexistence of a continuous P–SWC–ET pathway and an episodic P–Rf–GW pathway provides direct empirical evidence of variable coupling states across events (Figure 9). Specifically, the threshold behavior observed in SWC responses and the activation of recharge only during large precipitation events (>78 mm) are consistent with the hypothesis that coupling is strengthened by increases in total water availability and connectivity among soil and subsurface domains (McDowell et al., 2023; Wilcox et al., 2022; Moreno-De-Las-Heras et al., 2020). Conversely, the absence of groundwater response during smaller P events, despite measurable increases in SWC and ET, indicates partial decoupling between near-surface water pools and deeper flow paths, supporting the idea that these domains can remain hydraulically disconnected under low

https://doi.org/10.5194/egusphere-2026-6044
Preprint. Discussion started: 5 November 2026
© Author(s) 2026. CC BY 4.0 License.

moisture conditions (Schwinning et al., 2004; Mayor et al., 2011). In addition, the rapid Rf generation followed by immediate groundwater responses suggests that preferential flow paths act as transient connectors between shallow and deep water pools, in line with the hypothesis that macropore flow and event-scale infiltration dynamics regulate coupling strength (McDowell et al. 2023; Castelli et al., 2019; Chappell and Tych, 2012). While McDowell et al. (2023) primarily frame these processes in the context of disturbance-driven changes in vegetation and energy balance, our results demonstrate that similar coupling–decoupling dynamics can emerge in undisturbed karst systems as a function of P event magnitude, antecedent SWC conditions, and subsurface structure. Thus, the framework developed from our study's findings extends those of prior work by showing that ecohydrological coupling is not only a function of disturbance and succession, but also an intrinsic property of pulse-driven dryland systems governed by threshold-dependent connectivity (Niborski et al., 2026; Magliano et al., 2023; Búrquez et al., 2024).

From a water management perspective, the episodic nature of recharge in the Edwards Plateau poses significant challenges for predicting GW sustainability under changing climatic and land use conditions (Piemontese et al., 2020; Sadeghi et al., 2020; Huang and Wilcox 2005; Chen et al., 2001; Loáiciga et al., 2000). Because recharge is controlled by a small number of high-magnitude P events, variations in the frequency and intensity of such events can have disproportionate effects on long-term water availability. This sensitivity is particularly relevant in the context of projected climate change. Land management practices further complicate this picture because they influence vegetation structure and soil properties, which in turn regulate ET and SWC (Vivoni et al., 2021; Zhao et al., 2010). The two major anthropogenic forcings that take place in the Edwards Plateau are: woody plant encroachment and urbanization. Woody plant encroachment increases both canopy interception (Gignac et al., 2025; Magliano et al., 2019) and ET (Wilcox and Huang 2010; Huxman et al., 2005) and thereby reduces Rf generation (Londe et al., 2022; Huxman et al., 2005; Wilcox et al., 2003)—the combination of these three processes resulting in the need for more (and more frequent) large P events to sustainably recharge GW. Urbanization may reduce SWC and increase Rf generation (Magliano et al., 2026; Guerra and Debbage 2021), with the result that GW recharge may be activated by smaller P events.

In summary, our findings demonstrate that recharge processes in the Edwards Plateau—and in karst systems more generally—is governed by episodic connectivity rather than continuous fluxes. Under these conditions, a limited number of hydrologically effective P events exert a dominant control on long-term water availability (see Figure 9). Consequently, management approaches based on mean conditions or steady-state assumptions are unlikely to capture karst system dynamics. Instead, for predicting aquifer status, it is critical to anticipate changes in the frequency and magnitude of recharge-generating P events and how these are modulated by land surface properties (Figure 9). This framework is directly transferable to karst landscapes worldwide, in all of which vertical preferential flow and rapid

https://doi.org/10.5194/egusphere-2026-6044
Preprint. Discussion started: 5 November 2026
© Author(s) 2026. CC BY 4.0 License.

subsurface connectivity amplify the sensitivity of recharge to event-scale processes. If management practices are to adequately address karst-system recharge dynamics under ongoing climatic and land use change, it will be essential to incorporate threshold behavior and event-based connectivity into water resource planning.

5. Conclusions

Our study shows that water fluxes in the Edwards Plateau are dynamically coupled through non-linear and threshold-dependent ecohydrological processes operating across different temporal scales. Our findings showed that P inputs were partitioned between two contrasting but interconnected pathways. The first pathway, linking P, SWC, and ET, behaves as a relatively continuous and buffered system controlled primarily by atmospheric demand and transient soil water storage. The second pathway, linking P, Rf, and GW, operates episodically and is activated only during a limited number of large P events capable of generating hydrological connectivity between surface and subsurface compartments. These findings support a conceptual framework in which ecohydrological coupling in semiarid karst systems is governed by intermittent windows of hydrological connectivity activated only when P pulses overcome both atmospheric demand and internal storage thresholds. Under this framework, Rf and GW recharge represent coupled expressions of the same connectivity process, differing primarily in temporal persistence and storage integration.

Code availability

No custom software or model code was developed as part of this study. Statistical analyses were performed using standard statistical procedures as described in the Methods section.

Data availability

The data supporting the findings of this study include precipitation, soil water content, evapotranspiration, runoff, and groundwater-level records from the Field Research Park, Texas, USA. The datasets were obtained from the Edwards Aquifer Authority and the FLUXNET network

Author contribution

PNM conceived the study, performed the data analysis, prepared the figures, and wrote the original draft of the manuscript. PAML: conceived the study. HGO: conceived the study.

https://doi.org/10.5194/egusphere-2026-6044
Preprint. Discussion started: 5 November 2026
© Author(s) 2026. CC BY 4.0 License.

BPW: conceived and supervised the study. All authors contributed to the interpretation of the results, reviewed and edited the manuscript, and approved the final version.

Competing interests

The authors declare that they have no conflict of interest.

Acknowledgements

This work was made possible thanks to the collaboration of the Edwards Aquifer Authority. All data used were obtained from the Field Research Park. The authors express special gratitude for the collaboration of Brent Doty, Mark Hamilton, Logan Schmidt, and Thomas Marsalia. We also thank Yuri Jacques for his collaboration on the first field trips and Vivi Hriscu for his technical assistance with the manuscript. The authors used ChatGPT (OpenAI) for English-language editing and improvement of text clarity. All scientific analyses, interpretations, and conclusions were developed and verified by the authors.

Financial support

This study was entirely supported by the Edwards Aquifer Authority of Texas. Award number: 26-009-AMS.

References

Asbjornsen, H., Goldsmith, G. R., Alvarado-Barrientos, M. S., Rebel, K., Van Osch, F. P., Rietkerk, M., ... and Dawson, T. E: Ecohydrological advances and applications in plant–water relations research: a review, Journal of Plant Ecology, 4, 3-22, 2011. https://doi.org/10.1093/jpe/rtr005

Baker, A., Scheller, M., Oriani, F., Mariethoz, G., Hartmann, A., Wang, Z., and Cuthbert, M. O: Quantifying temporal variability and spatial heterogeneity in rainfall recharge thresholds in a montane karst environment, Journal of Hydrology, 594, 125965, 2021. https://doi.org/10.1016/j.jhydrol.2021.125965

Baldocchi, D. D., Wilson, K. B., and Gu, L: How the environment, canopy structure and canopy physiological functioning influence carbon, water and energy fluxes of a temperate broad-leaved deciduous forest—an assessment with the biophysical model CANOAK, Tree Physiology, 22, 1065-1077, 2002. https://doi.org/10.1093/treephys/22.15-16.1065

https://doi.org/10.5194/egusphere-2026-6044
Preprint. Discussion started: 5 November 2026
© Author(s) 2026. CC BY 4.0 License.

Basant, S., B. P. Wilcox, P. M. Leite, and C. L. Morgan: When Savannas Recover from Overgrazing, Ecohydrological Connectivity Collapses, Environmental Research Letters, 15, 054001, 2020. https://doi.org/10.1088/1748-9326/ab71a1

Bautista, S., and A. G. Mayor: El papel de la (des) conectividad ecohidrologica en el funcionamiento y el manejo de las zonas áridas, Ecosistemas: Revista Cietifica y Tecnica de Ecologia y Medio Ambiente, 30, 2265–5, 2021. https://doi.org/10.7818/ECOS.2265

Berdugo, M., Delgado-Baquerizo, M., Soliveres, S., Hernández-Clemente, R., Zhao, Y., Gaitán, J. J., ... and Maestre, F. T: Global ecosystem thresholds driven by aridity, Science, 367, 787-790, 2020. https://doi.org/10.1126/science.aay5958

Búrquez, A., M. B. Ochoa, A. Martínez-Yrízar, and J. O. P. de Souza: Human-Made Small Reservoirs Alter Dryland Hydrological Connectivity, Science of the Total Environment, 947, 174673, 2024. https://doi.org/10.1016/j.scitotenv.2024.174673

Canton, Y., A. Solé-Benet, J. De Vente, C. Boix-Fayos, A. Calvo-Cases, C. Asensio, and J. Puigdefabregas: A Review of Runoff Generation and Soil Erosion across Scales in Semiarid South- Eastern Spain, Journal of Arid Environments, 75, 1254–61, 2011. https://doi.org/10.1016/j.jaridenv.2011.03.004

Calvo-Cases, A., Arnau-Rosalén, E., Boix-Fayos, C., Estrany, J., Roxo, M. J., and Symeonakis, E: Eco-geomorphological connectivity and coupling interactions at hillslope scale in drylands: Concepts and critical examples, Journal of Arid Environments, 186, 104418, 2021. https://doi.org/10.1016/j.jaridenv.2020.104418

Castelli, G., L. Oliveira, F. Abdelli, H. Dhaou, E. Bresci, and M. Ouessar: Effect of Traditional Check Dams (Jessour) on Soil and Olive Trees Water Status in Tunisia, Science of the Total Environment, 690, 226–236, 2019. https://doi.org/10.1016/j.scitotenv.2019.06.514

Chappell, N. A., and Tych, W: Identifying step changes in single streamflow and evaporation records due to forest cover change, Hydrological Processes, 26, 100-116, 2012. https://doi.org/10.1002/hyp.8115

Chamizo, S., Y. Cantón, E. Rodríguez-Caballero, F. Domingo, and A. Escudero: Runoff at Contrasting Scales in a Semiarid Ecosystem: A Complex Balance Between Biological Soil Crust Features and Rainfall Characteristics, Journal of Hydrology, 452, 130–138, 2012. https://doi.org/10.1016/j.jhydrol.2012.05.045

Chen, C. C., Gillig, D., and McCarl, B. A: Effects of climatic change on a water dependent regional economy: a study of the Texas Edwards aquifer, Climatic Change, 49, 397-409, 2001. https://link.springer.com/article/10.1023/A:1010617531401#preview

D'Odorico, P., A. Bhattachan, K. F. Davis, S. Ravi, and C. W. Runyan: Global Desertification: Drivers and Feedbacks, Advances in Water Resources, 51, 326–44, 2013. https://doi.org/10.1016/j.advwatres.2012.01.013

Dunkerley, D: Light and Low-Intensity Rainfalls: A Review of their Classification, Occurrence, and Importance in Landsurface, Ecological and Environmental Processes, Earth- Science Reviews, 214, 103529, 2021. https://doi.org/10.1016/j.earscirev.2021.103529

https://doi.org/10.5194/egusphere-2026-6044
Preprint. Discussion started: 5 November 2026
© Author(s) 2026. CC BY 4.0 License.

Elkington, R. J., Rebel, K. T., Heilman, J. L., Litvak, M. E., Dekker, S. C., and Moore, G. W: Species-specific water use by woody plants on the Edwards Plateau, Texas, Ecohydrology, 7, 278-290, 2014. https://doi.org/10.1002/eco.1344

Estaville, L. E., and Earl, R. A: Texas water atlas, Texas A&M University Press, 2008. https://books.google.com.ar/books?hl=es&lr=&id=HAOn2QdqfF0C&oi=fnd&pg=PP13&dq=Texas+water+atlas,+Texas+A%26M+University+&ots=-SyyKpS1uD&sig=yLO33kvmlCcJ3D5MB-7VNwF-Rw8&redir_esc=y#v=onepage&q=Texas%20water%20atlas%2C%20Texas%20A%26M%20University&f=false

Ferrill, D. A., Sims, D. W., Waiting, D. J., Morris, A. P., Franklin, N. M., and Schultz, A. L: Structural framework of the Edwards Aquifer recharge zone in south-central Texas, Geological Society of America Bulletin, 116, 407-418, 2004. https://doi.org/10.1130/B25174.1

Fowler, N. L: An introduction to the vegetation and ecology of the eastern Edwards Plateau (Hill Country) of Texas, Edward's Plateau Ecology, 1-16, 2005. https://www.researchgate.net/profile/Norma-Fowler/publication/255621459_An_Introduction_to_the_Vegetation_and_Ecology_of_the_Eastern_Edwards_Plateau_Hill_Country_of_Texas/links/0c96053b56a80289aa000000/An-Introduction-to-the-Vegetation-and-Ecology-of-the-Eastern-Edwards-Plateau-Hill-Country-of-Texas.pdf

Gignac, J. E., Basant, S., Leite, P. A., and Wilcox, B. P: Thicketization by Yaupon Holly Increases Canopy Interception in the Texas Post Oak Savannah, Rangeland Ecology and Management, 103, 431-440, 2025. https://doi.org/10.1016/j.rama.2025.07.013

Gnatowski, T., Szatyłowicz, J., Pawluśkiewicz, B., Oleszczuk, R., Janicka, M., Papierowska, E., and Szejba, D: Field calibration of TDR to assess the soil moisture of drained peatland surface layers, Water, 10, 1842, 2018. https://doi.org/10.3390/w10121842

Guerra, J. F., and Debbage, N: Changes in urban land use throughout the Edwards Aquifer: A comparative analysis of Austin, San Antonio, and the Interstate–35 corridor, Applied Geography, 133, 102480, 2021. https://doi.org/10.1016/j.apgeog.2021.102480

Gustavson, T. C: Bed forms and stratification types of modern gravel meander lobes, Nueces River, Texas, Sedimentology, 25, 401-426, 1978. https://doi.org/10.1111/j.1365-3091.1978.tb00319.x

Hartmann, A., Goldscheider, N., Wagener, T., Lange, J., and Weiler, M: Karst water resources in a changing world: Review of hydrological modeling approaches, Reviews of Geophysics, 52, 218-242, 2014. https://doi.org/10.1002/2013RG000443

Hervé-Fernández, P., Oyarzún, C., Brumbt, C., Huygens, D., Bodé, S., Verhoest, N. E. C., and Boeckx, P. J. H. P: Assessing the 'two water worlds' hypothesis and water sources for native and exotic evergreen species in south-central Chile, Hydrological Processes, 30, 4227-4241, 2016. https://doi.org/10.1002/hyp.10984

https://doi.org/10.5194/egusphere-2026-6044
Preprint. Discussion started: 5 November 2026
© Author(s) 2026. CC BY 4.0 License.

Hernandez, E. A., and Uddameri, V: Standardized precipitation evaporation index (SPEI)-based drought assessment in semi-arid south Texas, Environmental Earth Sciences, 71, 2491-2501, 2014. https://doi.org/10.1007/s12665-013-2897-7

Gregory, L., Wilcox, B. P., Shade, B., Munster, C., Owens, K., and Veni, G: Large-scale rainfall simulation over shallow caves on karst shrublands, Ecohydrology: Ecosystems, Land and Water Process Interactions, Ecohydrogeomorphology, 2, 72-80, 2009. https://doi.org/10.1002/eco.41

Heilman, J. L., Litvak, M. E., McInnes, K. J., Kjelgaard, J. F., Kamps, R. H., and Schwinning, S: Water-storage capacity controls energy partitioning and water use in karst ecosystems on the Edwards Plateau, Texas, Ecohydrology, 7, 127-138, 2014. https://doi.org/10.1002/eco.1327

Heilman, J. L., McInnes, K. J., Kjelgaard, J. F., Owens, M. K., and Schwinning, S: Energy balance and water use in a subtropical karst woodland on the Edwards Plateau, Texas, Journal of Hydrology, 373, 426-435, 2009. https://doi.org/10.1016/j.jhydrol.2009.05.007

Huang, Y., and Wilcox, B. P: How Karst features affect recharge? Implication for estimating recharge to the Edwards aquifer, In Sinkholes and the Engineering and Environmental Impacts of Karst (pp. 201-206), 2005. https://doi.org/10.1061/40796(177)21

Huxman, T. E., Snyder, K. A., Tissue, D., Leffler, A. J., Ogle, K., Pockman, W. T., ... and Schwinning, S: Precipitation pulses and carbon fluxes in semiarid and arid ecosystems, Oecologia, 141, 254-268, 2004. https://doi.org/10.1007/s00442-004-1682-4

Huxman, T. E., Wilcox, B. P., Breshears, D. D., Scott, R. L., Snyder, K. A., Small, E. E., ... and Jackson, R. B: Ecohydrological implications of woody plant encroachment, Ecology, 86, 308-319, 2005. https://doi.org/10.1890/03-0583

Jobbágy, E. G., Nosetto, M. D., Santoni, C. S., and Baldi, G: El desafío ecohidrológico de las transiciones entre sistemas leñosos y herbáceos en la llanura Chaco-Pampeana, Ecología austral, 18, 305-322, 2008. https://ojs.ecologiaaustral.com.ar/index.php/Ecologia_Austral/article/view/1377/743

Loáiciga, H. A., Maidment, D. R., and Valdes, J. B: Climate-change impacts in a regional karst aquifer, Texas, USA, Journal of Hydrology, 227, 173-194, 2000. https://doi.org/10.1016/S0022-1694(99)00179-1

Leite, P. A., Schmidt, L. M., Rempe, D. M., Olariu, H. G., Walker, J. W., McInnes, K. J., and Wilcox, B. P: Woody plant encroachment modifies carbonate bedrock: field evidence for enhanced weathering and permeability, Scientific Reports, 13, 15431, 2023. https://doi.org/10.1038/s41598-023-42226-7

Leite, P. A., B. P. Wilcox, and K. J. McInnes: Woody Plant Encroachment Enhances Soil Infiltrability of a Semiarid Karst Savanna, Environmental Research Communications, 2, 115005, 2020. https://doi.org/10.1088/2515-7620/abc92f

Leite, P. A., E. S. de Souza, E. S. dos Santos, R. J. Gomes, J. R. Cantalice, and B. P. Wilcox: The Influence of Forest Regrowth on Soil Hydraulic Properties and Erosion in a Semiarid Region of Brazil, Ecohydrology, 11, e1910, 2018. https://doi.org/10.1002/eco.1910

https://doi.org/10.5194/egusphere-2026-6044
Preprint. Discussion started: 5 November 2026
© Author(s) 2026. CC BY 4.0 License.

784 Litvak, M. E., Schwinning, S., and Heilman, J. L: Woody plant rooting depth and ecosystem
785 function of savannas: a case study from the Edwards Plateau Karst, Texas, Ecosystem
786 Function in savannas, 117, 134, 2011.
787 https://www.taylorfrancis.com/chapters/edit/10.1201/b10275-15/woody-plant-rooting-
788 depth-ecosystem-function-savannas-case-study-edwards-plateau-karst-texas-marcy-
789 litvak-susan-schwinning-james-heilman

790 Londe, D. W., Cady, S. M., Elmore, R. D., and Fuhlendorf, S. D: Woody plant encroachment
791 pervasive across three socially and ecologically diverse ecoregions, Ecology and
792 Society, 27(3), 2022. https://doi.org/10.5751/ES-13348-270311

793 Ludwig, J. A., Wilcox, B. P., Breshears, D. D., Tongway, D. J., and Imeson, A. C: Vegetation
794 patches and runoff–erosion as interacting ecohydrological processes in semiarid
795 landscapes, Ecology, 86, 288-297, 2005. https://doi.org/10.1890/03-0569

796 Maestre, F. T., Eldridge, D. J., Soliveres, S., Kéfi, S., Delgado-Baquerizo, M., Bowker, M.
797 A., ... and Berdugo, M: Structure and functioning of dryland ecosystems in a changing
798 world, Annual review of ecology, evolution, and systematics, 47, 215-237, 2016.
799 https://doi.org/10.1146/annurev-ecolsys-121415-032311

800 Magliano, P. N., Breshears, D. D., Fernández, R. J., and Jobbágy, E. G: Rainfall intensity
801 switches ecohydrological runoff/runon redistribution patterns in dryland vegetation
802 patches, Ecological applications, 25, 2094-2100, 2015. https://doi.org/10.1890/15-
803 0550.1

804 Magliano, P. N., Breshears, D. D., Murray, F., Niborski, M. J., Nosetto, M. D., Zou, C. B.,
805 and Jobbágy, E. G: South American Dry Chaco rangelands: Positive effects of cattle
806 trampling and transit on ecohydrological functioning, Ecological Applications, 33, e2800,
807 2023. https://doi.org/10.1002/eap.2800

808 Magliano, P. N., Castelli, G., Niborski, M. J., Piemontese, L., Petit, M. V., Anichini, F., ... and
809 Jobbágy, E. G: Disentangling a century of water harvesting development in the
810 Paraguayan dry Chaco flatlands, Hydrological Sciences Journal, 71(8), 1539-1548,
811 2026. https://doi.org/10.1080/02626667.2026.2654775

812 Magliano, P. N., Fernández, R. J., Giménez, R., Marchesini, V. A., Páez, R. A., and Jobbágy,
813 E. G: Cambios en la partición de flujos de agua en el Chaco Árido al reemplazar bosques
814 por pasturas, Ecología austral, 26, 95-106, 2016.
815 https://ojs.ecologiaaustral.com.ar/index.php/Ecologia_Austral/article/view/148

816 Magliano, P. N., Whitworth-Hulse, J. I., and Baldi, G: Interception, throughfall and stemflow
817 partition in drylands: Global synthesis and meta-analysis, Journal of Hydrology, 568,
818 638-645, 2019. https://doi.org/10.1016/j.jhydrol.2018.10.042

819 Mayor, AG., S. Bautista, and J. Bellot: Scale-Dependent Variation in Runoff and Sediment
820 Yield in a Semiarid Mediterranean Catchment, Journal of Hydrology, 397, 128–35, 2011.
821 https://doi.org/10.1016/j.jhydrol.2010.11.039

822 McDowell, N. G., Anderson-Teixeira, K., Biederman, J. A., Breshears, D. D., Fang, Y.,
823 Fernandez-de-Una, L., ... and Chen, X: Ecohydrological decoupling under changing

https://doi.org/10.5194/egusphere-2026-6044
Preprint. Discussion started: 5 November 2026
© Author(s) 2026. CC BY 4.0 License.

disturbances and climate, One Earth, 6, 251-266, 2023. https://doi.org/10.1016/j.oneear.2023.02.007

McMillan, H: Linking hydrologic signatures to hydrologic processes: A review, Hydrological Processes, 34, 1393-1409, 2020. https://doi.org/10.1002/hyp.13632

Moreno-De-Las-Heras, M., L. Merino-Martín, P. M. Saco, T. Espigares, F. Gallart, and J. M. Nicolau: Structural and Functional Control of Surface-Patch to Hillslope Runoff and Sediment Connectivity in Mediterranean Dry Reclaimed Slope Systems, Hydrology and Earth System Sciences, 24, 2855–72, 2020. https://doi.org/10.5194/hess-24-2855-2020

Morrissey, P., Nolan, P., McCormack, T., Johnston, P., Naughton, O., Bhatnagar, S., and Gill, L: Impacts of climate change on groundwater flooding and ecohydrology in lowland karst. Hydrology and Earth System Sciences, 25, 1923-1941, 2021. https://doi.org/10.5194/hess-25-1923-2021

Niborski, M. J., Murray, F., Jobbágy, E. G., Fernández, R. J., Nosetto, M. D., Páez, R. A., ... and Magliano, P. N: The Elusive Runoff Generation: Understanding Thresholds and Pathways in a Dry Sedimentary Plain, Hydrological Processes, 40, e70399, 2026. https://doi.org/10.1002/hyp.70399

Nielsen-Gammon, J. W., Banner, J. L., Cook, B. I., Tremaine, D. M., Wong, C. I., Mace, R. E., ... and Kloesel, K: Unprecedented drought challenges for Texas water resources in a changing climate: what do researchers and stakeholders need to know?, Earth's Future, 8, e2020EF001552, 2020. https://doi.org/10.1029/2020EF001552

Nosetto, M. D., Luna Toledo, E., Magliano, P. N., Figuerola, P., Blanco, L. J., and Jobbagy, E. G: Contrasting CO2 and water vapour fluxes in dry forest and pasture sites of central Argentina, Ecohydrology, 13, e2244, 2020. https://doi.org/10.1002/eco.2244

Noy-Meir, I: Desert ecosystems: environment and producers, Annual review of ecology and systematics, 25-51, 1973. https://doi.org/10.1146/annurev.es.04.110173.000325

Olariu, H. G., Wilcox, B. P., and Popescu, S. C: Linking woody plants, climate, and evapotranspiration in a temperate savanna, Hydrology and Earth System Sciences, 29, 4825-4846, 2025. https://doi.org/10.5194/hess-29-4825-2025

Piemontese, L., G. Castelli, I. Fetzer, et al: Estimating the Global Potential of Water Harvesting From Successful Case Studies, Global Environmental Change, 63, 102121, 2020. https://doi.org/10.1016/j.gloenvcha.2020.102121

Reynolds, J. F., Kemp, P. R., Ogle, K., and Fernández, R. J: Modifying the 'pulse–reserve' paradigm for deserts of North America: precipitation pulses, soil water, and plant responses, Oecologia, 141, 194-210, 2004. https://doi.org/10.1007/s00442-004-1524-4

Rantz, S. E., et al: Measurement and computation of streamflow, U.S. Geological Survey Water-Supply Paper 2175, 1982. https://books.google.com.ar/books?hl=es&lr=&id=A0n9rm9NJ2UC&oi=fnd&pg=PA285&dq=Measurement+and+computation+of+streamflow,+&ots=nsuLcM3jrB&sig=lJQLMWePLT2raC53w_7aLU1x8rs&redir_esc=y#v=onepage&q=Measurement%20and%20computation%20of%20streamflow%2C&f=false

https://doi.org/10.5194/egusphere-2026-6044
Preprint. Discussion started: 5 November 2026
© Author(s) 2026. CC BY 4.0 License.

Saco, P. M., J. F. Rodríguez, M. Moreno-de las Heras, S. Keesstra, S. Azadi, S. Sandi, J. Baartman, J. Rodrigo-Comino, and M. J. Rossi: Using Hydrological Connectivity to Detect Transitions and Degradation Thresholds: Applications to Dryland Systems, Catena, 186, 104354, 2020. https://doi.org/10.1016/j.catena.2019.104354

Sadeghi, S. M. M., Gordon, D. A., and Van Stan II, J. T: A global synthesis of throughfall and stemflow hydrometeorology, In Precipitation partitioning by vegetation: A global synthesis (pp. 49-70). Cham: Springer International Publishing, 2020. https://link.springer.com/chapter/10.1007/978-3-030-29702-2_4

Scanlon, B. R., Keese, K. E., Flint, A. L., Flint, L. E., Gaye, C. B., Edmunds, W. M., and Simmers, I: Global synthesis of groundwater recharge in semiarid and arid regions, Hydrological Processes: An International Journal, 20, 3335-3370, 2006. https://doi.org/10.1002/hyp.6335

Schwinning, S., Sala, O. E., Loik, M. E., and Ehleringer, J. R: Thresholds, memory, and seasonality: understanding pulse dynamics in arid/semi-arid ecosystems, Oecologia, 141, 191-193, 2004. https://doi.org/10.1007/s00442-004-1683-3

Schwantes, A. M., Swenson, J. J., González-Roglich, M., Johnson, D. M., Domec, J. C., and Jackson, R. B: Measuring canopy loss and climatic thresholds from an extreme drought along a fivefold precipitation gradient across Texas, Global Change Biology, 23, 5120-5135, 2017. https://doi.org/10.1111/gcb.13775

Schwartz, B. F., Schwinning, S., Gerrard, B., Kukowski, K. R., Stinson, C. L., and Dammeyer, H. C: Using hydrogeochemical and ecohydrologic responses to understand epikarst process in semi-arid systems, Edwards Plateau, Texas, USA, Acta Carsologica, 42(2-3), 2013. https://ojs.zrc-sazu.si/carsologica/article/view/670

Seneviratne, S. I., Corti, T., Davin, E. L., Hirschi, M., Jaeger, E. B., Lehner, I., ... and Teuling, A. J: Investigating soil moisture–climate interactions in a changing climate: A review, Earth-Science Reviews, 99, 125-161, 2010. https://doi.org/10.1016/j.earscirev.2010.02.004

Shao, Q., and Campbell, N. A: Applications: Modelling trends in groundwater levels by segmented regression with constraints, Australian and New Zealand Journal of Statistics, 44, 129-141, 2002. https://doi.org/10.1111/1467-842X.00216

Sharp, J. M., and Banner, J. L: The Edwards Aquifer: Water for Thirsty Texans, In The Earth Around Us (pp. 154-165). Routledge, 2018. https://www.taylorfrancis.com/chapters/edit/10.4324/9780429496653-16/edwards-aquifer-water-thirsty-texans-john-sharp-jay-banner

Smeins, F. E., Taylor, T. W., and Merrill, L. B: Vegetation of a 25-year exclosure on the Edwards Plateau, Texas, Journal of Range Management, 29, 24-29, 1976. https://repository.arizona.edu/bitstream/handle/10150/650436/12732-13423-1-PB.pdf?sequence=1#page=28

Thurow, T. L., Blackburn, W. H., and Taylor, C. A: Hydrologic characteristics of vegetation types as affected by livestock grazing systems, Edwards Plateau, Texas, 1986.

https://doi.org/10.5194/egusphere-2026-6044
Preprint. Discussion started: 5 November 2026
© Author(s) 2026. CC BY 4.0 License.

https://repository.arizona.edu/bitstreams/129ab40e-d6d1-4ce6-933d-56f3d330ae77/download

Toomey III, R. S., Blum, M. D., and Valastro Jr, S: Late Quaternary climates and environments of the Edwards Plateau, Texas, Global and planetary change, 7, 299-320, 1993. https://doi.org/10.1016/0921-8181(93)90003-7

Turnbull, L., Wainwright, J., and Brazier, R. E: A conceptual framework for understanding semi-arid land degradation: Ecohydrological interactions across multiple-space and time scales, Ecohydrology: Ecosystems, Land and Water Process Interactions, Ecohydrogeomorphology, 1, 23-34, 2008. https://doi.org/10.1002/eco.4

Turnipseed, D. P., and Sauer, V. B: Discharge measurements at gaging stations, U.S. Geological Survey Techniques and Methods 3–A8, 2010. https://pubs.usgs.gov/publication/tm3A8

Van Stan, J. T., and Pinos, J: Three fundamental challenges to the advancement of stemflow research and its integration into natural science, Water, 16, 117, 2023. https://doi.org/10.3390/w16010117

Vanderlinden, K., Vereecken, H., Hardelauf, H., Herbst, M., Martínez, G., Cosh, M. H., and Pachepsky, Y. A: Temporal stability of soil water contents: A review of data and analyses, Vadose Zone Journal, 11, vzj2011-0178, 2012. https://doi.org/10.2136/vzj2011.0178

Villegas, J. C., Breshears, D. D., Zou, C. B., and Law, D. J: Ecohydrological controls of soil evaporation in deciduous drylands: How the hierarchical effects of litter, patch and vegetation mosaic cover interact with phenology and season, Journal of Arid Environments, 74, 595-602, 2010. https://doi.org/doi:10.1016/j.jaridenv.2009.09.028

Vivoni, E. R., E. R. Pérez-Ruiz, Z. T. Keller, E. A. Escoto, R. C. Templeton, N. P. Templeton, C. A. Anderson, A. P. Schreiner- McGraw, L. A. Méndez-Barroso, and A. Robles-Morua: Long-Term Research Catchments to Investigate Shrub Encroachment in the Sonoran and Chihuahuan Deserts: Santa Rita and Jornada Experimental Ranges, Hydrological Processes, 35, e14031, 2021. https://doi.org/10.1002/hyp.14031

Wang, L., d'Odorico, P., Evans, J. P., Eldridge, D. J., McCabe, M. F., Caylor, K. K., and King, E. G: Dryland ecohydrology and climate change: critical issues and technical advances, Hydrology and Earth System Sciences, 16, 2585-2603, 2012. https://doi.org/10.5194/hess-16-2585-2012

Whitworth-Hulse, J. I., Magliano, P. N., Zeballos, S. R., Nosetto, M. D., Gurvich, D. E., Ferreras, A., ... and Kowaljow, E: Ligustrum lucidum invasion alters the soil water dynamic in a seasonally multi-specific dry forest, Forest Ecology and Management, 549, 121493, 2023. https://doi.org/10.1016/j.foreco.2023.121493

Wilcox, B. P., S. Basant, H. Olariu, and P. A. Leite: Ecohydrological Connectivity: A Unifying Framework for Understanding How Woody Plant Encroachment Alters the Water Cycle in Drylands, Frontiers in Environmental Science, 10, 934535, 2022. https://doi.org/10.3389/fenvs.2022.934535

https://doi.org/10.5194/egusphere-2026-6044
Preprint. Discussion started: 5 November 2026
© Author(s) 2026. CC BY 4.0 License.

Wilcox, B. P., Breshears, D. D., and Allen, C. D: Ecohydrology of a resource-conserving semiarid woodland: Effects of scale and disturbance, Ecological monographs, 73, 223-239, 2003. https://doi.org/10.1890/0012-9615

Wilcox, B. P., and Huang, Y: Woody plant encroachment paradox: Rivers rebound as degraded grasslands convert to woodlands, Geophysical Research Letters, 37(7), 2010. https://doi.org/10.1029/2009GL041929

Wilcox, B. P., Taucer, P. I., Munster, C. L., Owens, M. K., Mohanty, B. P., Sorenson, J. R., and Bazan, R: Subsurface stormflow is important in semiarid karst shrublands, Geophysical Research Letters, 35(10), 2008. https://doi.org/10.1029/2008GL033696

Wilcox, B. P., Wilding, L. P., and Woodruff Jr, C. M: Soil and topographic controls on runoff generation from stepped landforms in the Edwards Plateau of Central Texas, Geophysical Research Letters, 34(24), 2007. https://doi.org/10.1029/2007GL030860

Zhang, Y., Feng, X., Zhou, C., Sun, C., Leng, X., and Fu, B: Aridity threshold of ecological restoration mitigated atmospheric drought via land–atmosphere coupling in drylands, Communications Earth and Environment, 5, 381, 2024. https://doi.org/10.1038/s43247-024-01555-9

Zhao, Y., Peth, S., Krümmelbein, J., Horn, R., Wang, Z., Steffens, M., ... & Peng, X. (2007). Spatial variability of soil properties affected by grazing intensity in Inner Mongolia grassland. Ecological modelling, 205(1-2), 241-254. https://doi.org/10.1016/j.ecolmodel.2007.02.019

Zhao, Y., Peth, S., Horn, R., Krümmelbein, J., Ketzer, B., Gao, Y., ... & Peng, X. (2010). Modeling grazing effects on coupled water and heat fluxes in Inner Mongolia grassland. Soil and Tillage Research, 109(2), 75-86. https://doi.org/10.1016/j.still.2010.04.005

Zuur, A. F., Ieno, E. N., Walker, N. J., Saveliev, A. A., and Smith, G. M: Mixed effects models and extensions in ecology with R (Vol, 574, p. 574). New York: springer, 2009. https://link.springer.com/book/10.1007/978-0-387-87458-6